

Seismic performance evaluation of staggered wall system structures with middle corridors

Joonho Lee, Hyungoo Kang and Jinkoo Kim*†

Department of Architectural Engineering, Sungkyunkwan University, Suwon, Korea

SUMMARY

In this paper, the seismic performance of reinforced concrete (RC) staggered wall structures with middle corridor was evaluated. To this end, 6-, 12- and 18-storey structural models were designed and were analyzed to investigate the seismic load-resisting capacity. The response modification factors were computed based on the overstrength and the ductility capacities obtained from pushover curves. The effect of a few retrofit schemes on the enhancement of strength and ductility was also investigated. The pushover analysis results showed that the response modification factors ranged between about 4.0 and 6.0 with the average value around 5.0. When the bending rigidity of the link beams increased up to 100%, the overall overstrength increased by only about 25%. When the rebar ratio of the link beams was increased by 50%, the overstrength increased by about 40%. The replacement of the RC link beams with steel box beams resulted in superior performance of the structures with reduced beam depth. The displacement time histories of the model structures subjected to the earthquake ground motions scaled to the design seismic load showed that the maximum interstorey drifts were well below the limit state specified in the design code. Based on the analysis results, it was concluded that the staggered wall systems with a middle corridor had enough capacity to resist the design seismic load. Copyright © 2012 John Wiley & Sons, Ltd.

Received 20 September 2011; Accepted 11 November 2011

KEYWORDS: staggered wall systems; seismic performance; response modification factors

1. INTRODUCTION

The staggered wall system (SWS) structure is composed of a series of storey-high reinforced concrete (RC) walls spanning the total width between two rows of exterior columns and arranged in a staggered pattern on adjacent column lines. Fintel (1968) carried out analytical and experimental study of the SWS with a web opening and found that it possessed many architectural and planning advantages, which proved to be more economical than the conventional systems. Mee *et al.* (1975) obtained dynamic properties of the system through both modal analysis and shaking table test. The staggered systems were originally developed in Massachusetts Institute of Technology as steel staggered truss systems (Scalzi, 1971). The system is known to have advantages such as low floor-to-floor heights, large column-free spaces, increased design flexibility, fast erection time and reduced weight of the superstructure and therefore reduced foundation cost. The staggered truss systems have been successfully applied to many large-scale building projects (Mcknamara, 1999; Pollak, 2004). For seismic performance evaluation of staggered truss systems, Kim *et al.* (2007) carried out a nonlinear analysis of staggered truss systems and found that plastic hinges formed at the horizontal and vertical chords of the Vierendeel panels, which subsequently led to the brittle collapse of the structure. Zhou *et al.* (2009) conducted an experimental investigation on the behavior of an eight-storey steel staggered truss system with a 1/8-scaled model under reversed low cyclic loading and investigated their performance indices such as ductility, energy dissipation and rigidity degeneration. Compared with the

*Correspondence to: Jinkoo Kim, Department of Architectural Engineering, Sungkyunkwan University, Suwon, Korea.

†E-mail: jkim12@skku.edu

staggered truss system, the SWS in RC has not been widely investigated. Recently, Kim and Jun (2011) investigated the seismic performance of partially staggered wall apartment buildings using nonlinear static and dynamic analysis and compared the results with the responses of conventional shear wall system apartment buildings.

In this study, the seismic performance of RC SWS structures with a middle corridor was evaluated. To this end, 6-, 12- and 16-storey SWS structural models were designed and were analyzed by nonlinear static analyses to obtain their force–displacement relationship up to failure. The response modification factors were computed based on the overstrength and the ductility capacities obtained from the capacity envelopes. Finally, the seismic responses of the model structures subjected to three earthquake ground motions were evaluated by nonlinear dynamic analysis.

2. DESIGN OF ANALYSIS MODEL STRUCTURES

2.1. Configuration of the analysis model structures

In the SWSs, the storey-high RC walls that span the width of the building are located along the short direction in a staggered pattern (Figure 1). The floor system spans from the top of one staggered wall to the bottom of the adjacent wall serving as a diaphragm. The staggered walls with attached slabs resist the gravity as well as the lateral loads as H-shaped deep beams. The horizontal load is transferred to the staggered walls below through diaphragm action of floor slabs. In this study, the staggered walls were designed as storey-high deep beams. With RC walls located at alternate floors, flexibility in spatial planning can be achieved compared with conventional wall-type structures with vertically continuous shear walls. Figure 1 shows the flow of horizontal shear force from the staggered walls above to the columns and staggered walls below through floor diaphragm. Figure 2 shows the deformation of the SWSs with middle corridor

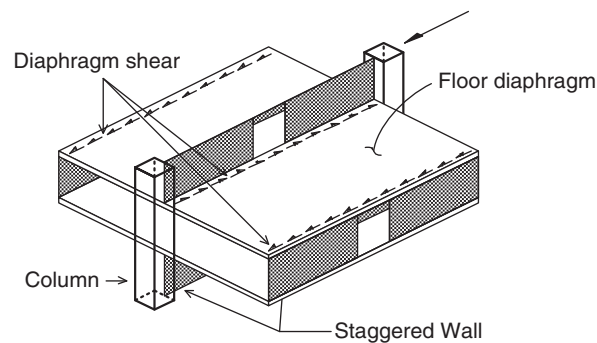


Figure 1. Lateral load path of SWS.

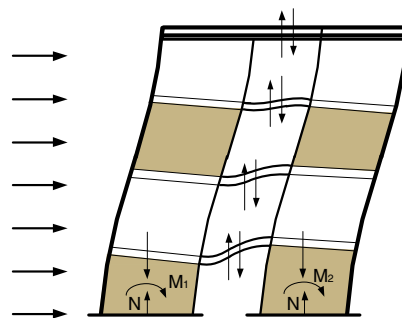


Figure 2. Lateral deformation of SWS with a middle corridor.

subjected to lateral load. As the exterior columns and the link beams above the openings along the corridors are significantly weaker and more flexible than the storey-high walls, large deformation is concentrated in the beams and columns. This leads to shear mode behavior when the system is subjected to lateral load.

Figure 3 shows the structural plan and 3-D configuration of the model structures. Columns and beams are located along the longitudinal perimeter of the structures providing a full width of column-free area within the structure. Along the longitudinal direction, the column-beam combination resists lateral load as a moment resisting frame. Figure 4 shows the side view of the model structure.

2.2. Structural design of analysis model structures

The staggered truss or SWSs have not been considered as one of the basic seismic-force-resisting systems in most design codes. Federal Emergency Management Agency (FEMA)-450 (BSSC, 2002) requires that lateral systems that are not listed as the basic seismic-force-resisting systems shall be permitted if analytical and test data are submitted to demonstrate the lateral force resistance and energy dissipation capacity. The American Institute of Steel Construction (AISC, 2002) Design Guide 14 recommends the response modification factor of 3.0 for seismic design of staggered truss system buildings; however, the other seismic behavior factors, such as overstrength and ductility factors, to define inelastic behavior of the structure are not specified.

To evaluate the seismic performance of SWS structures, 6-, 12- and 18-storey structural models were designed and were named as SWC06, SWC12 and SWC18, respectively. The model structures were designed as per the ACI 318-06 (ACI, 2005) using the seismic loads specified in the International Building Code 2009 (ICC, 2009). For gravity loads, the dead and live loads of 7 kN/m^2 and 2 kN/m^2 were used, respectively. The design seismic load was computed based on

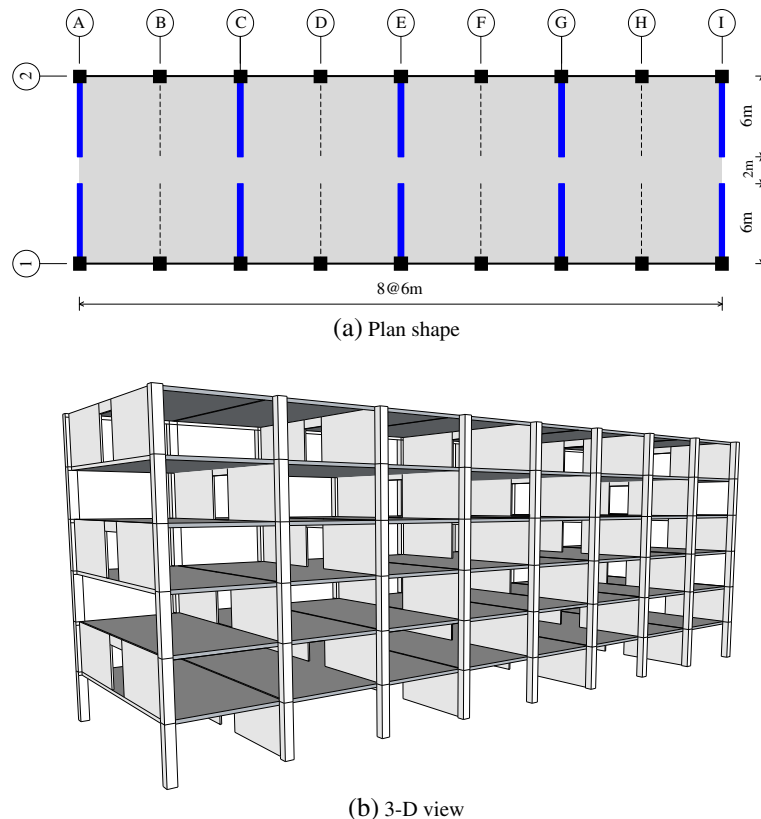


Figure 3. Shape of the SWS model structures.

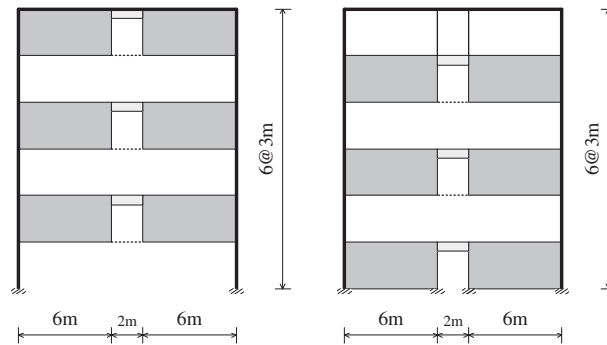


Figure 4. Side view of SWS.

the design spectral response acceleration parameters $S_{DS}=0.31\text{ g}$ and $S_{D1}=0.13\text{ g}$. This corresponds to the design seismic load in Los Angeles (LA) area with site class B, which is a rock site. Because the response modification factor for an SWS is not specified in the current design codes, the response modification factor of 3.0 was used in the structural design of the SWSs, which is generally used for the structures to be designed without consideration of seismic detailing. Along the longitudinal direction, the structures were designed as ordinary moment resisting frames with R -factor of 3.0. The ultimate strength of concrete is 27 MPa, and the tensile strength of rebars is 400 MPa. The thickness of the staggered walls is 20 cm throughout the stories, and the connecting beams have the size of $200 \times 600\text{ mm}$. The thickness of the floor slabs is 21 cm, which is the minimum thickness required for wall-type apartment buildings in Korea to prevent transmission of excessive noise and vibration through the floors. Tables 1 to 3 show the dimensions and rebars of the analysis model structures.

2.3. Modeling for analysis

The displacement-controlled pushover analyses were conducted using the nonlinear analysis/design program code MIDAS (MIDAS, 2011) to obtain the nonlinear load–displacement relationships of the model structures. The lateral loading profiles for the pushover analysis were determined proportional to the fundamental mode shapes of the model structures. The staggered walls were modeled by the top and bottom rigid beam elements and the vertical line element

Table 1. Sectional properties of staggered walls.

Section	Thickness(mm)	Vertical	Horizontal
Wall (SW06)	200	D13@200	D13@200
Wall (SW12)	200	D13@200	D13@200
Wall (SW18)	200	D13@200	D13@200

Table 2. Sectional properties of link beams.

Section	Size (mm)	Stirrup	Rebar			
			Exterior (I, J)		Interior (M)	
			Bottom	Top	Bottom	Top
LB(SW06)	200×600	D13@100	4-D22	4-D22	2-D22	2-D22
LB(SW12)	200×600	D13@100	4-D25	4-D25	2-D25	2-D25
LB(SW18)	200×600	D13@100	4-D29	4-D29	2-D25	2-D25

Table 3. Sectional properties of columns.

Section	Size (mm)	Rebar	Section	Size (mm)	Rebar
SWC06-B1	600 × 600	6-D32	SWC18-B1	900 × 900	20-D35
SWC06-B2	580 × 580	6-D29	SWC18-B2	880 × 880	20-D32
SWC06-B3	560 × 560	6-D29	SWC18-B3	860 × 860	20-D29
SWC06-B4	540 × 540	6-D25	SWC18-B4	840 × 840	20-D29
SWC06-B5	520 × 520	6-D25	SWC18-B5	820 × 820	20-D25
SWC06-B6	500 × 500	6-D25	SWC18-B6	800 × 800	18-D25
SWC12-B1	760 × 760	14-D35	SWC18-B7	780 × 780	18-D22
SWC12-B2	740 × 740	14-D32	SWC18-B8	760 × 760	18-D22
SWC12-B3	720 × 720	14-D29	SWC18-B9	740 × 740	16-D22
SWC12-B4	700 × 700	14-D25	SWC18-B10	720 × 720	16-D22
SWC12-B5	680 × 680	12-D22	SWC18-B11	700 × 700	16-D22
SWC12-B6	660 × 660	12-D22	SWC18-B12	680 × 680	12-D22
SWC12-B7	640 × 640	12-D22	SWC18-B13	660 × 660	12-D22
SWC12-B8	620 × 620	10-D22	SWC18-B14	640 × 640	12-D22
SWC12-B9	600 × 600	10-D22	SWC18-B15	620 × 620	10-D22
SWC12-B10	580 × 580	10-D22	SWC18-B16	600 × 600	10-D22
SWC12-B11	560 × 560	10-D22	SWC18-B17	580 × 580	10-D22
SWC12-B12	540 × 540	8-D22	SWC18-B18	560 × 560	10-D22

composed of the nonlinear axial, flexural and shear springs as shown in Figure 5. The middle line element behaves like a 3-D beam-column element, and the top and bottom rigid beams act as rigid bodies in the $x-z$ plane. The moments about the Z -axis represent the in-plane bending behavior, and the out-of-plane bending behavior was not considered in the wall element. The expected ultimate strengths of the concrete and steel were taken to be 1.5 and 1.25 times the nominal strengths based on the recommendation of the FEMA-356 (2000). The slabs were considered as rigid diaphragm, and the p -delta effect was considered in the analysis.

The nonlinear force-deformation relationship of the structural members recommended in the FEMA-356 (2000), which is shown in Figure 6(a), was used in the pushover analysis. In the idealized skeleton curve, linear response is depicted between point A and an effective yield point B . The slope from B to C represents strain hardening. In this study, the postyield stiffness was set to be 2% of the initial stiffness. C has an ordinate that represents the maximum strength of the component and has an abscissa value equal to the deformation at which significant strength degradation begins (line CD). Beyond point D , the component responds with substantially reduced strength to point E . At deformations greater than point E , the component strength is essentially zero. The parameters a , b , c , d and e that are required for modeling structural components can be obtained from Tables 6-7 and 6-8 of the FEMA-356. The performance points, such

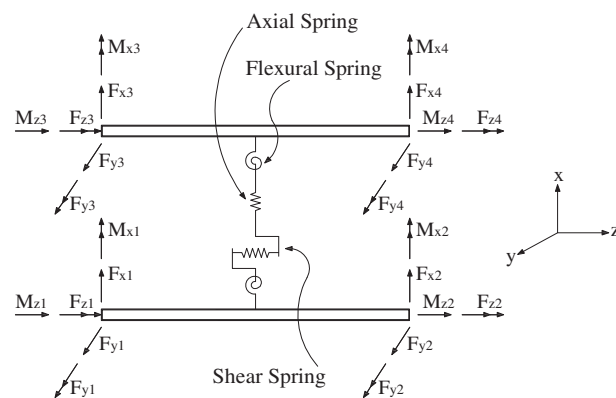


Figure 5. Modeling of staggered walls for pushover analysis.

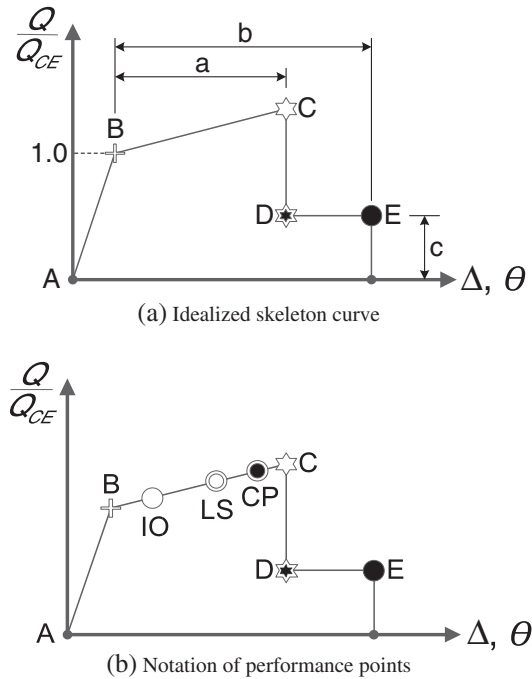


Figure 6. Generalized force–deformation relationship of an RC structural member defined in FEMA-356.

as immediate occupancy (IO), life safety (LS), collapse prevention (CP) and collapse (C), which are indicated in Figure 6(b), are also defined in the FEMA-356 report.

3. MAXIMUM STRENGTH AND INTERSTOREY DRIFT OF THE MODEL STRUCTURES

To evaluate the behavior factors of the model structures subjected to seismic load, pushover analyses were carried out along the transverse direction by applying incremental lateral load with its vertical profile proportional to the fundamental mode of vibration. The base shear versus roof displacement relationship for each model structure is depicted in Figure 7. Such information as the design base shear, the first yield points of the link beams and columns, the sudden strength drop and the points where the interstorey drift reached 1.5% of the storey height are also provided on the curves. It can be observed that the 18-storey structure showed the highest strength and lowest stiffness, and that the 6-storey structure showed the lowest strength but highest stiffness. In all structural models, the maximum strengths were higher than twice the design base shears. The major strength drop occurred before the maximum interstorey drift reached 1.5% of the storey height, which is generally considered as the limit state for the LS performance level. It was observed that the sudden drop of strength occurred due mainly to the formation of plastic hinges in the lower storey link beams.

Figure 8 depicts the interstorey drifts of the model structures when the strength dropped significantly and when the maximum interstorey drifts reached 1.5% of the storey height. It can be observed that the maximum interstorey drifts occurred at lower stories due to the formation of plastic hinges at the link beams between the staggered walls.

Figure 9 shows the storey shear–interstorey drift curves of the model structures. It can be observed that in all model structures, the storey stiffness and strength are generally higher in lower stories. The ductility demands are higher in lower stories, which corresponds well with the relative distribution of the interstorey drifts shown in Figure 6. Compared with the storey shear versus interstorey drift relationship curves of higher stories, the curves of lower stories generally show distinct yield points.

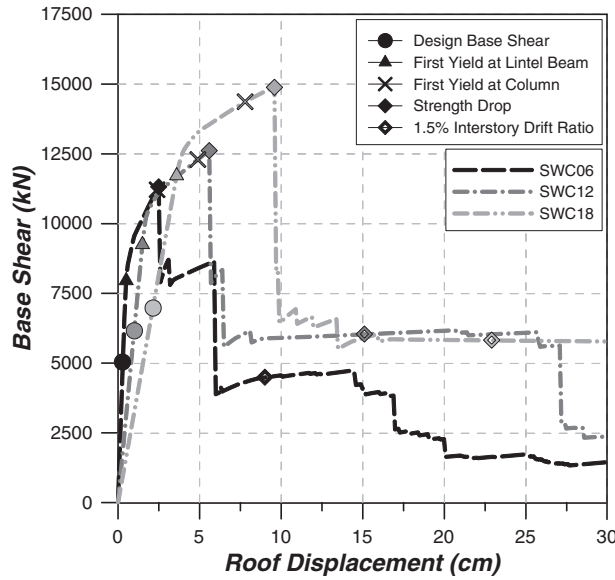


Figure 7. Nonlinear static pushover analysis.

Figures 10–12 depict the plastic hinge formation of the model structures when the strength dropped suddenly and when the maximum interstorey drift reaches 1.5% of the storey height. It was observed that the link beams in the lower stories yielded first followed by yielding of the lower storey columns. Only minor deformation occurred in the lower storey staggered walls, and the walls located in the higher stories generally remained elastic.

4. SEISMIC REINFORCEMENT OF STAGGERED WALL SYSTEMS

It was observed in the analysis that the significant strength degradation was initiated by yielding of link beams followed by yielding of the exterior columns. As reinforcing schemes for staggered wall structures, the following methods were used: (a) increase of the column size in such a way that its flexural stiffness is increased by 25%, 50%, 75% and 100%, (b) increase of the link beam depth in the same proportions, (c) replacement of RC link beams with steel box beams with 300 × 150 × 20 mm in size and (d) addition of interior columns with 200 × 300 mm and 200 × 400 mm in size at both sides of the corridor openings of the staggered walls. Figures 13 to 16 show the pushover curves of the three model structures redesigned with the reinforcing schemes mentioned above. In the first three retrofit cases, the collapse mechanisms of the retrofitted structures were similar to those of the original structures; most

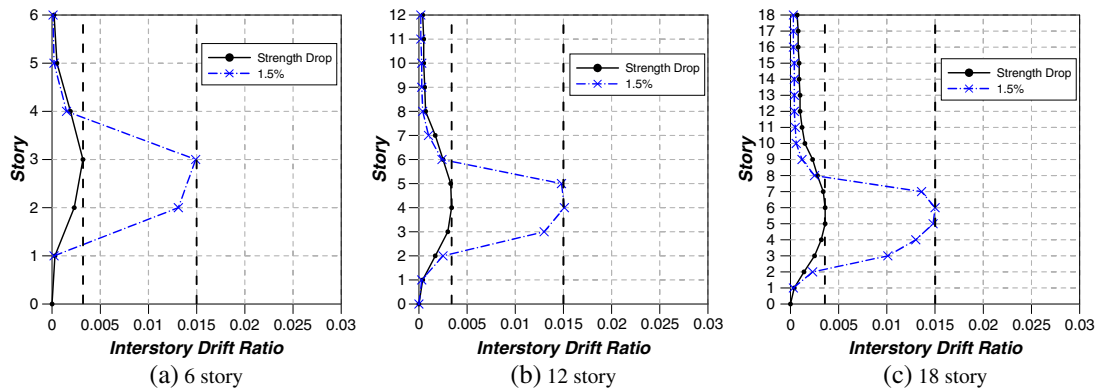


Figure 8. Interstorey drift ratios of the model structures.

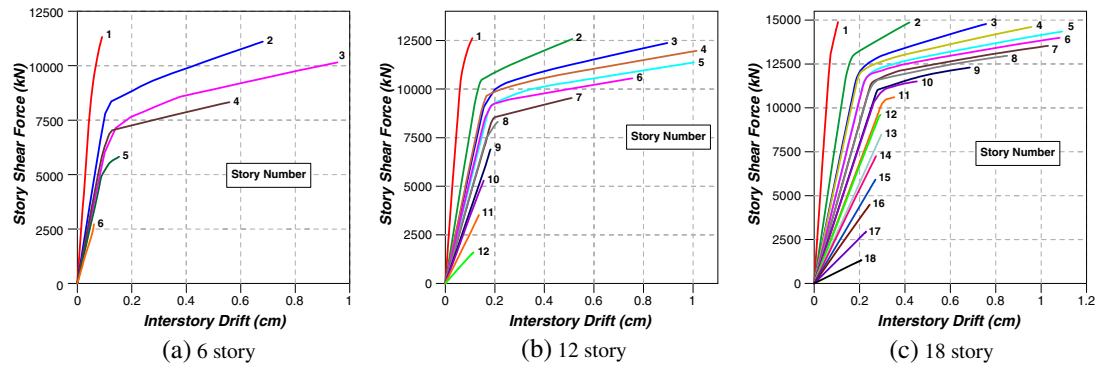


Figure 9. Relationship of storey shear versus interstorey drift.

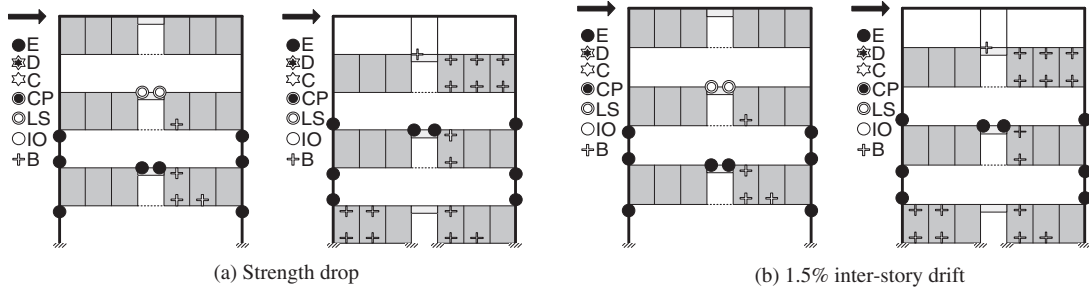


Figure 10. Plastic hinge formation at the points of sudden strength drop and at the 1.5% interstorey drift (six storeys).

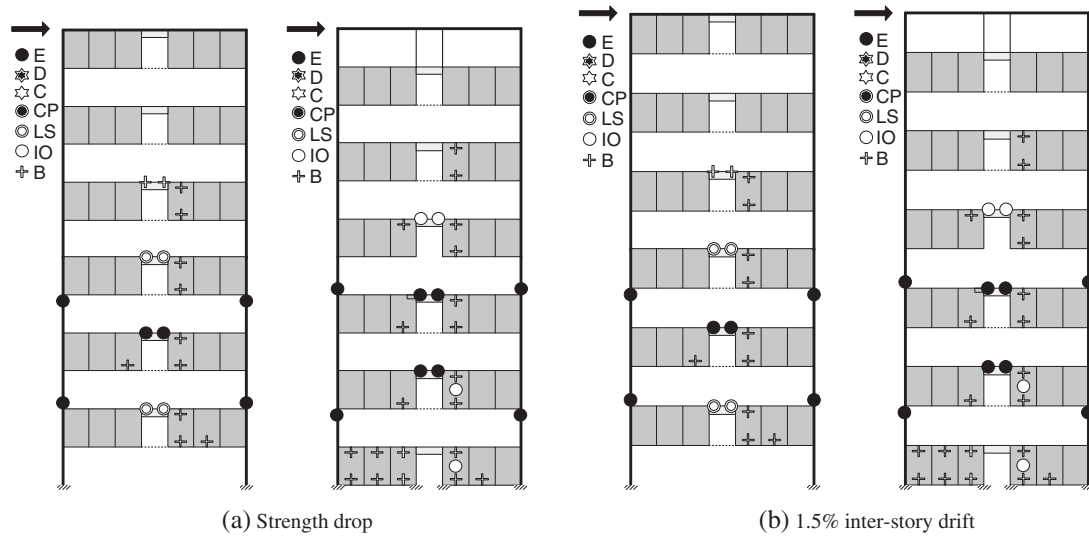


Figure 11. Plastic hinge formation at the points of sudden strength drop and at the 1.5% interstorey drift (12 storeys).

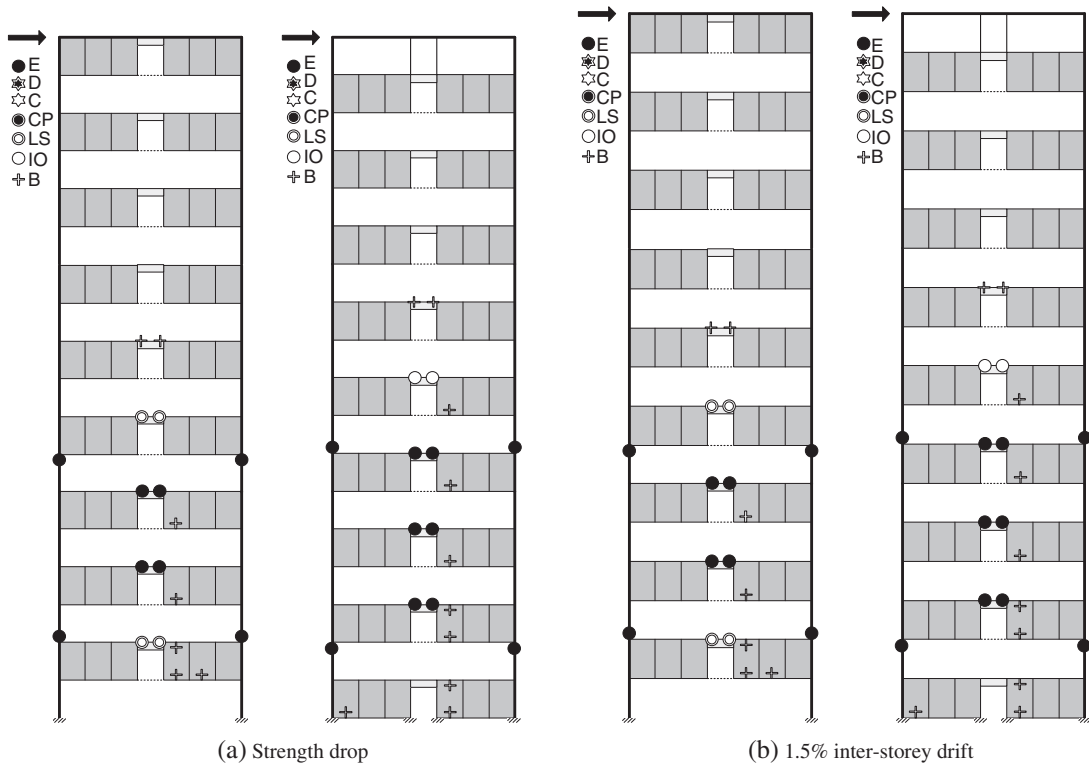


Figure 12. Plastic hinge formation at the points of sudden strength drop and at the 1.5% interstorey drift (18 storeys).

plastic hinges formed at lower storey link beams. However, when the interior columns were added, the plastic hinges spread to the higher stories, which resulted in significant increase in maximum strength. In all retrofit cases, the maximum strength somewhat increased, but the ductility did not increase significantly.

5. BEHAVIOR FACTORS OF THE STAGGERED WALL SYSTEM

The Applied Technology Council (ATC)-19 (1995) proposed simplified procedure to estimate the response modification factors by the product of the three parameters that profoundly influence the seismic response of structures:

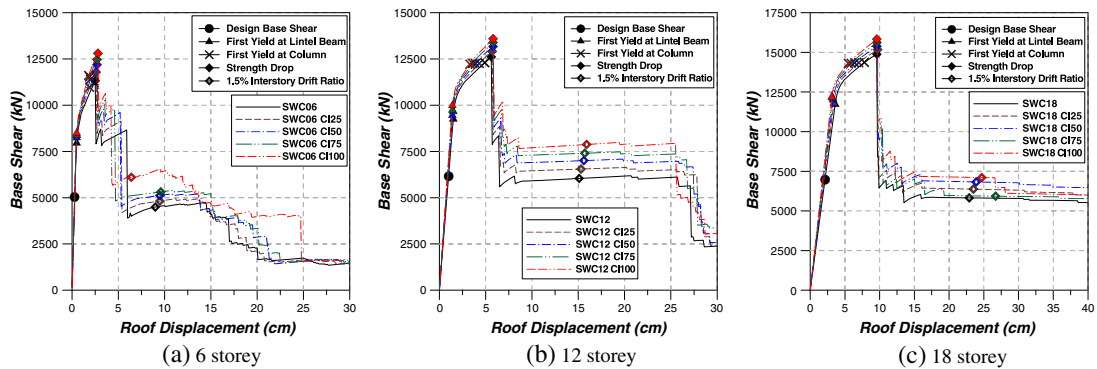


Figure 13. Base shear–roof displacement relationships of model structures with various column sizes.

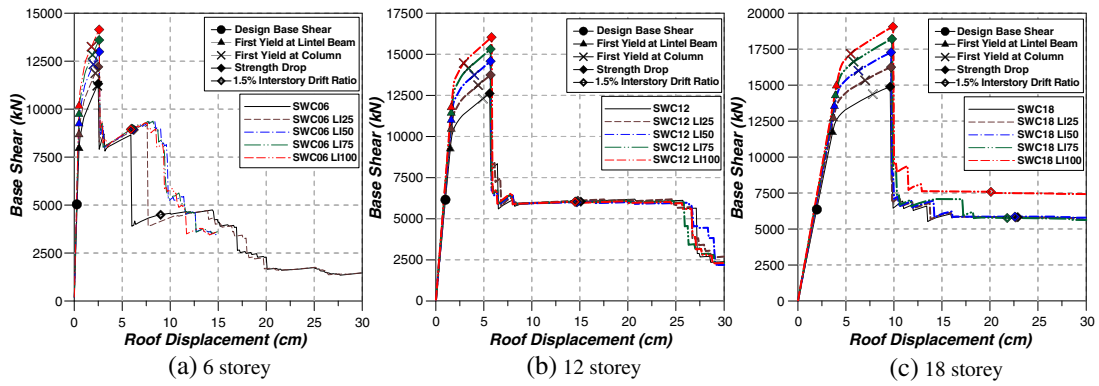


Figure 14. Base shear–roof displacement relationships of model structures with various link beam stiffness.

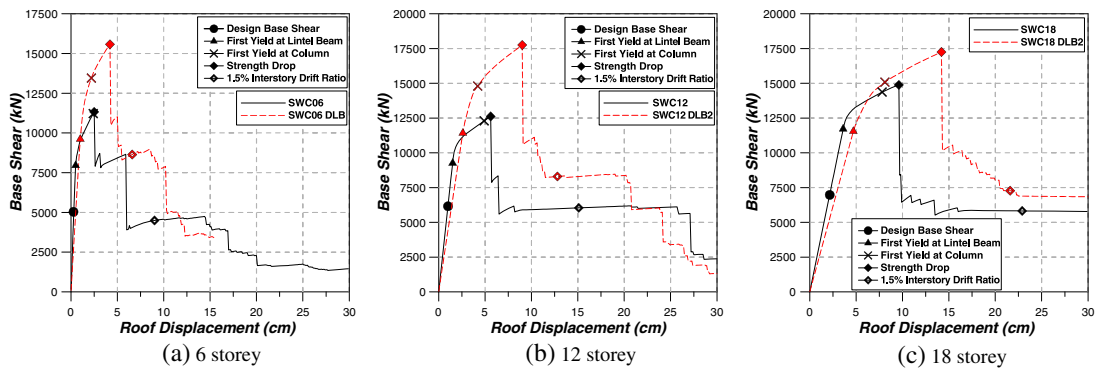


Figure 15. Base shear–roof displacement relationships of model structures with box-shaped steel link beam.

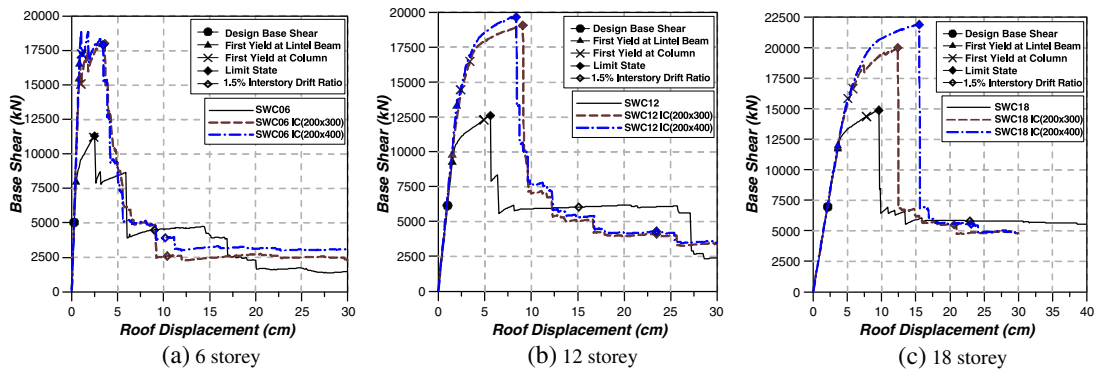


Figure 16. Base shear–roof displacement relationships of model structures with interior columns.

$$R = R_o R_\mu R_\gamma \tag{1}$$

where R_o is the overstrength factor to account for the observation that the maximum lateral strength of a structure generally exceeds its design strength. R_μ is a ductility factor that is a measure of the global nonlinear response of a structure, and R_γ is a redundancy factor to quantify the improved reliability of seismic framing systems constructed with multiple lines of strength. In this study, the redundancy factor was assumed to be 1.0 based on the fact that there are more than four seismic load-resisting frames

along the transverse direction. Then the response modification factor is determined as the product of the overstrength factor and the ductility factor. From the base shear versus roof displacement relationships, the overstrength factor and the ductility factor are obtained as follows (ATC-19, 1995):

$$R_o = \frac{V_y}{V_d}; R_\mu = \frac{V_e}{V_y} \tag{2a, b}$$

where V_d is the design base shear, V_e is the maximum seismic demand for elastic response and V_y is the base shear corresponding to the yield point, which can be obtained from the capacity curves. To find out the yield point, we drew straight lines on the pushover curve as shown in Figure 17 in such a way

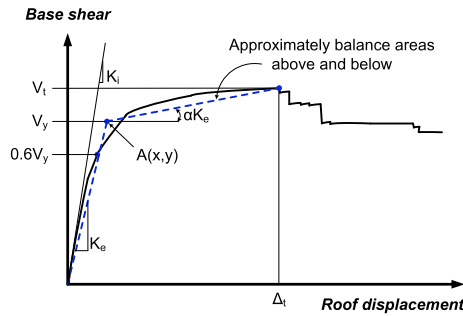


Figure 17. Idealization of load–displacement curve.

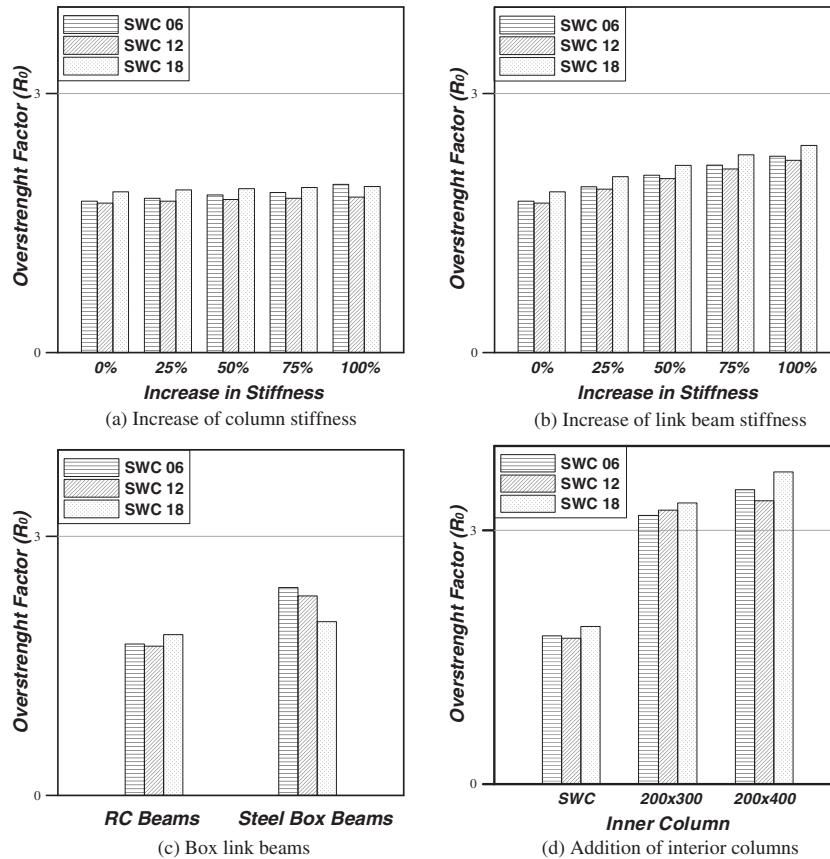


Figure 18. Overstrength factors of model structures with various retrofit schemes.

that the area under the original curve is equal to that of the idealized one as recommended in the FEMA-356 (2000).

The overstrength factors of the model structures were computed using Equation (2a) based on the pushover curves and are plotted in Figure 18. It can be observed that as in all model structures, the overstrength factors are slightly higher than 1.5, which is generally smaller than the structures designed with other structure systems. The increase in column size did not affect the overstrength factors significantly. When the flexural stiffness of the link beams was increased by 100%, the overstrength increased by 25%. When the interior columns were inserted, the overstrength increased significantly compared with those of the original structures.

Figure 19 plots the ductility factors of the model structures. The factors ranged approximately from two to three. It can be observed that ductility factors are generally inversely proportional to the number of stories. The various retrofit schemes applied to the original structures generally did not affect the ductility factors. Even though the addition of interior columns increased the failure points (the points with significant strength drop), the ductility factors remain unchanged due to the increased yield points.

The response modification factors are presented in Figure 20, which are computed by multiplying the overstrength and the ductility factors. It can be observed that the response modification factors range from four to six, higher than the code-recommended value for R -factor used in the structural design. This implies that the staggered wall structures with middle corridor may have enough resistance against the design level seismic load, and the code-recommended value for R -factor of 3.0 is reasonably determined. The six-storey model structure showed higher response modification factors than the taller structures. The R -factors of the structures designed with higher stiffness of exterior columns

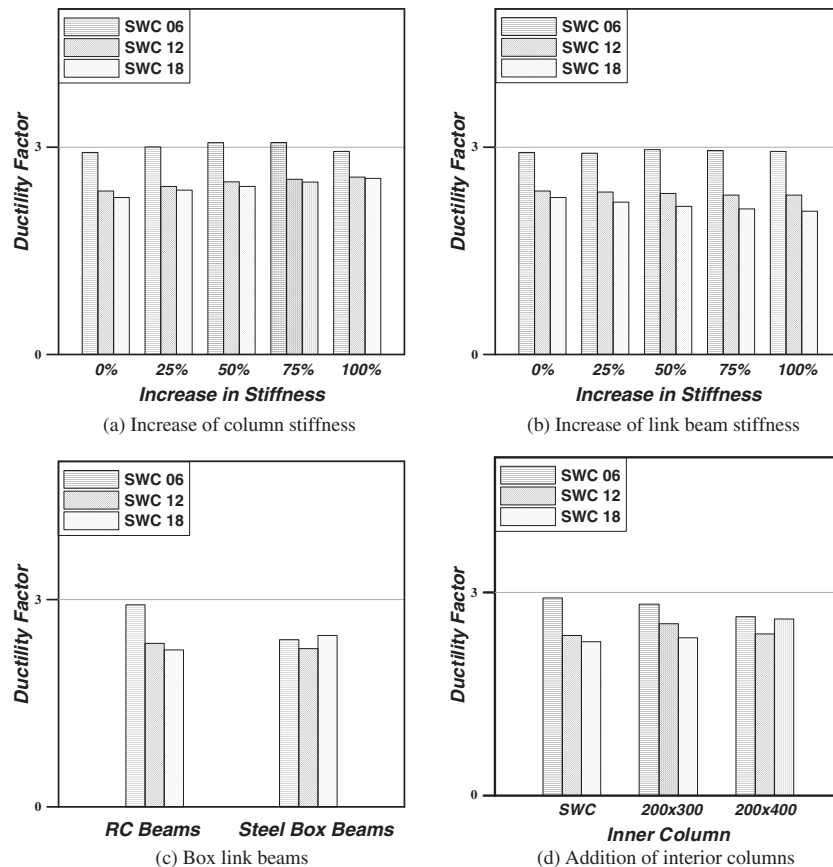


Figure 19. Ductility factors of model structures with various retrofit schemes.

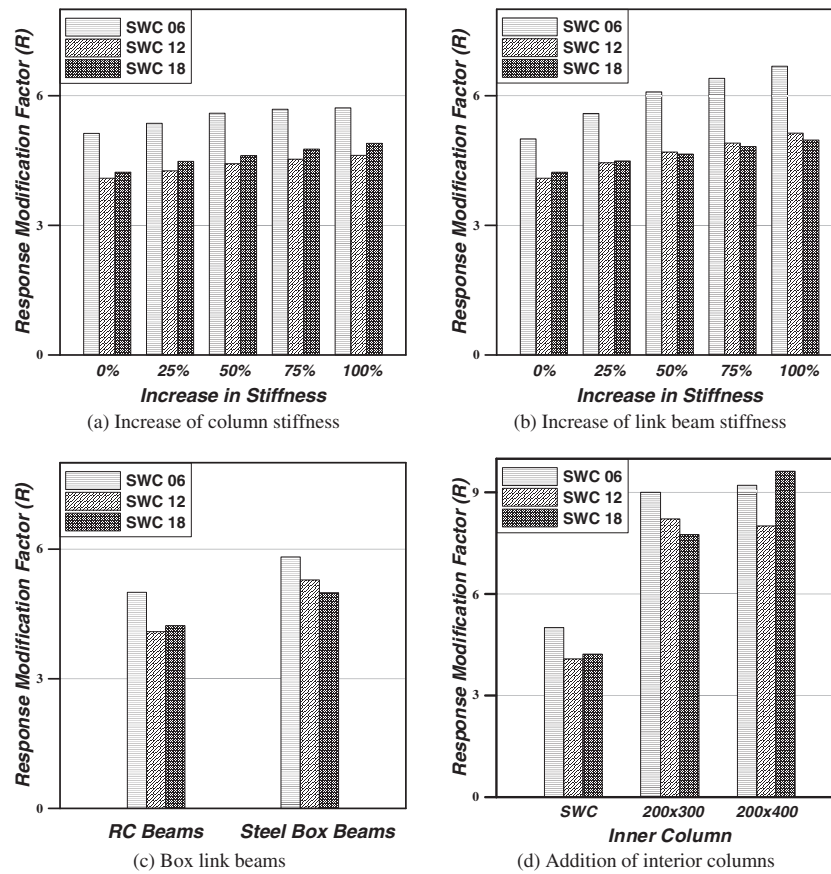


Figure 20. Response modification factors of model structures with various retrofit schemes.

and link beams are slightly higher than those of the original structures. The R -factors of the structures with steel box link beams increased about 10% compared with those of the original structures with RC link beams. The increase in R -factors is the most significant when the interior columns were added. In this case, the R -factors increased almost twice those of the original structures.

6. EVALUATION OF THE STRUCTURAL RESPONSES

The seismic performance of the SWS structures was evaluated by nonlinear dynamic analyses using the program code Perform 3D (Computers and Structures 2006) in which various types of nonlinear models including user-defined models were implemented for simulation of inelastic behavior of structures. The staggered walls were divided into many fiber elements, and the deformation such as fiber strains, hinge rotations and shear deformations was monitored using the axial and rotational gage elements.

The stress–strain relationship of concrete in the compression part was defined using the trilinear model proposed by Paulay and Priestley (1992), and the tensile strength was neglected. Because seismic detailing was not applied in the model structures, the confinement effect of rebars was not considered in the modeling of concrete. The maximum compressive strength (F_u) was assumed to be 27 MPa, and the yield and the residual strengths were assumed to be 60% and 20% of the maximum strength, respectively. The strain at the maximum strength and the ultimate strain were 0.002 and 0.004, respectively. Because a wall element has no in-plane rotational stiffness at its nodes, a beam element was imbedded in the wall to model the moment connection between staggered walls and the connecting link

beams. The behavior of rebars was modeled by bilinear lines with the postyield stiffness ratio of 0.02, and the behavior of the beams and the columns were modeled by the FEMA-356-type nonlinear models (Figure 21).

Dynamic time history analyses of the model structures were carried out to obtain the responses for the El Centro (NS), San Fernando (NS) and Taft (NS) earthquake ground motions. Figure 22 shows the response spectra of the earthquake records and the IBC 2009-based design spectrum with the spectral response acceleration parameters $S_{DS}=0.57\text{ g}$ and $S_{D1}=0.3\text{ g}$. The matching ground accelerations were scaled to have the effective peak accelerations of 0.227 g . This corresponds to the design seismic load in LA area with site class D. The displacement time histories of the model structure subjected to the three earthquake ground motions are presented in Figure 23. It can be noticed that at the end of the analysis, slight permanent displacement occurred, which implies that the structure experienced plastic deformation. However, the maximum interstorey drifts, shown in Figure 24, turned out to be far less than the limit state of 0.015 specified in the design code. Figure 25 shows the plastic hinge distribution of the 18-storey model structure subjected to the Taft earthquake when the maximum interstorey drift occurred. It can be observed that a few plastic hinges formed at the lower storey link beams, which is similar to the results obtained from the pushdown analysis. It was also observed that the magnitude of plastic rotation did not reach the LS performance objective specified in the FEMA-356.

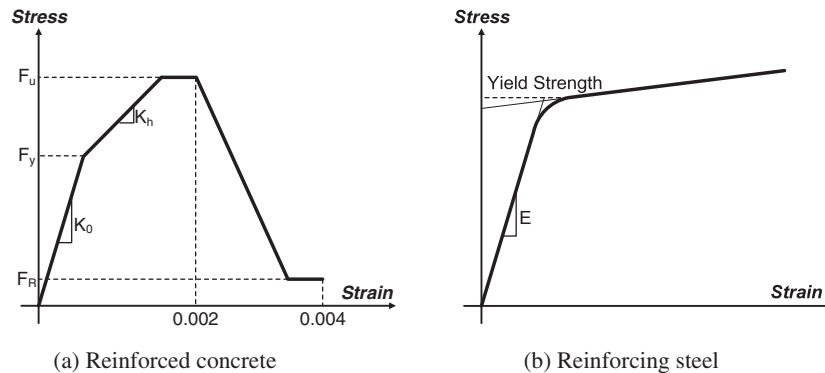


Figure 21. Nonlinear stress–strain relationship of structural materials.

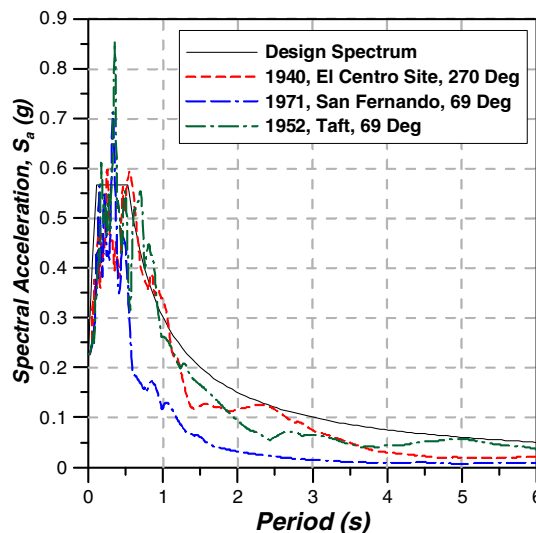


Figure 22. Response spectra of the scaled ground motions.

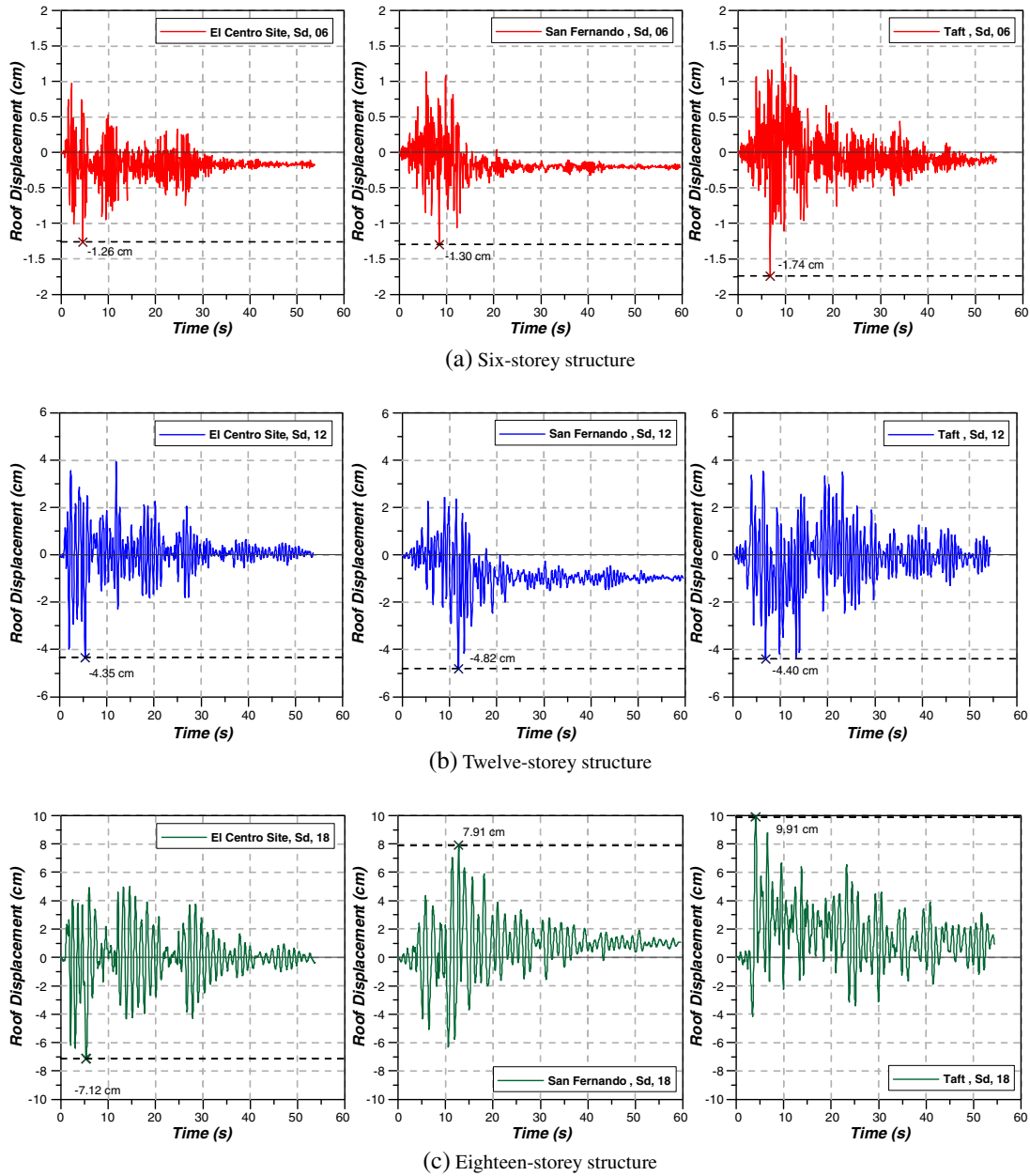


Figure 23. Time history of the roof storey displacement.

7. CONCLUSIONS

In this paper, the seismic performance of RC SWS structures with middle corridor was evaluated. To this end, 6-, 12- and 18-storey structural models were designed and were analyzed by pushover analysis to investigate the force–displacement relationship. The response modification factors were computed based on the overstrength and the ductility capacities obtained from the pushover curves.

The analysis results showed that plastic hinges formed first at the link beams located between two staggered walls and the structures failed by formation of weak stories. When the bending rigidity of the connection beams increased up to 100%, the overstrength increased by only about

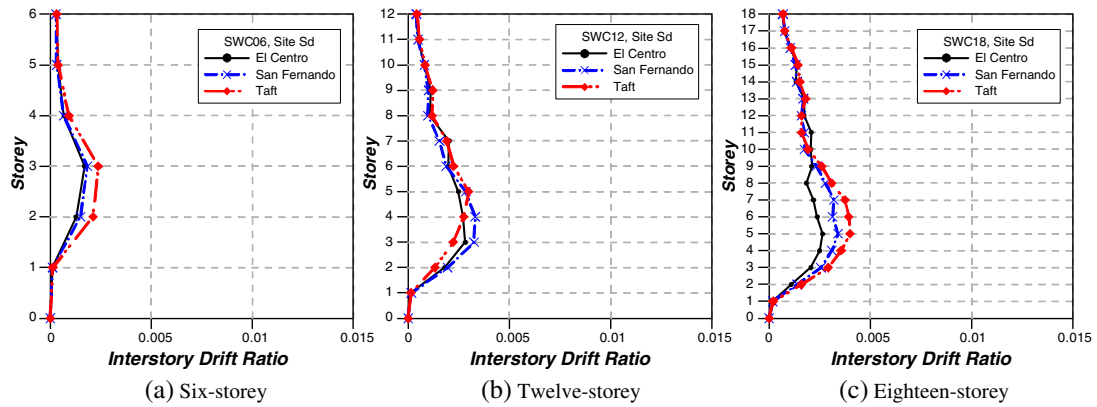


Figure 24. Maximum interstorey displacement of the model structures.

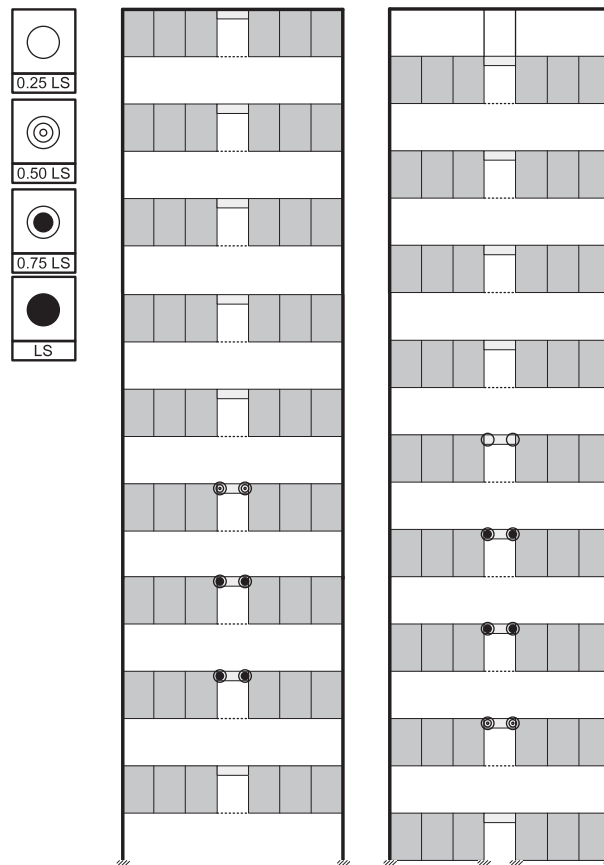


Figure 25. Plastic hinge formation in the 18-storey model obtained from nonlinear dynamic time history analysis using the Taft earthquake record.

25%. When the rebar ratio of the connection beams was increased by 50%, the overstrength increased by about 40%. The replacement of the RC connection beams with steel box beams resulted in superior performance of the structures with reduced beam depth. The response modification factors ranged between about 4.0 and 6.0 with the average value around 5.0. The dynamic time history analysis results showed that for the three earthquake ground motions, the maximum interstorey drifts turned out to be far less than the limit state of 0.015 specified in the design code. Based on these observations, it was concluded that the SWSs with a middle corridor had enough capacity to resist the design seismic load.

ACKNOWLEDGEMENT

This work (No. 2011-0015734) was supported by the Mid-career Researcher Program through National Research Foundation grant funded by the Korea Ministry of Education, Science and Technology.

REFERENCES

- ACI 318. 2005. Building code requirements for structural concrete and commentary (ACI 318M-05). American Concrete Institute, Farmington Hills, Michigan.
- AISC. 2002. Design Guide 14: Staggered Truss Framing Systems, American Institute of Steel Construction, Chicago, Illinois.
- ATC. 1995a. Structural response modification factors. ATC-19, Applied Technology Council, Redwood City, CA, 5–32.
- ATC. 1995b. A critical review of current approaches to earthquake-resistant design. ATC-34, Applied Technology Council, Redwood City, CA, 31–6.
- Computers and Structures, Inc. 2006. PERFORM Components and Elements for PERFORM 3D and PERFORM-Collapse Version 4. CSI, Berkeley, CA.
- FEMA. 2000. Prestandard and commentary for the seismic rehabilitation of buildings. FEMA-356, Federal Emergency Management Agency, Washington, DC.
- FEMA. 2002. NEHRP Recommended Provisions for Seismic Regulations for New Buildings and Other Structures, FEMA-450, Federal Emergency Management Agency, Washington, DC.
- Fintel AM. 1968. Staggered transverse wall-beams for multistory concrete buildings. *ACI Journal* 366–378.
- ICC. 2009. International code council. International Building Code, Falls Church, VA.
- Kim J, Jun Y. 2011. Seismic performance evaluation of partially staggered wall apartment buildings. *Magazine of Concrete Research*, **63**(12): 927–939.
- Kim J, Lee J, Kim Y. 2007. Inelastic behavior of staggered truss systems. *The Structural Design of Tall and Special Buildings* **16**(1): 85–105.
- Mcknamara RJ. 1999. Aladdin hotel, modern steel construction. American Institute of Steel Construction, May.
- Mee AL, Jordaan IJ, Ward MA. 1975. Dynamic response of a staggered wall-beam structure. *Earthquake Engineering and Structural Dynamics* **3**: 353–364.
- MIDAS. 2011. General structure design system for Window, Ver. 7.7.0.
- Paulay T, Priestley, MJN. 1992. *Seismic Design of Reinforced Concrete and Masonry Building*. John Wiley & Sons, Inc.: Hoboken, NJ.
- Pollak BS, Gustafson M. 2004. *Complex Apartments*. Modern Steel Construction: American Institute of Steel Construction, Fall
- Scalzi JB. 1971. The staggered truss system—structural considerations. *AISC Engineering Journal*, October.
- Zhou X, He Y, Xu L. 2009. Experimental study and numerical analyses on seismic behaviors of staggered truss system under low cyclic loads. *Thin-walled Structures* **47**(11): 1343–1353.

AUTHORS' BIOGRAPHIES

Mr. Joonho Lee received B.S. and M.S. degrees from the Department of Architectural Engineering, Sungkyunkwan University, Korea. Currently, he is a Ph.D. candidate in the same university.

Mr. Hyungoo Kang received his B.S. degree from the Department of Architectural Engineering, Yonnam University, Korea. Currently, he is a graduate student in Sungkyunkwan University.

Dr. Jinkoo Kim is a professor of Architectural Engineering at Sungkyunkwan University, Korea. He received his B.S. degree from the Seoul National University, Korea. His M.S. and Ph.D. degrees were from the Department of Civil and Environmental Engineering, Massachusetts Institute of Technology. His research interests include performance evaluation and retrofit of building structures against earthquake loads and progressive collapse.